

Quantum Dynamics of Pseudospin Solitons in Double-Layer Quantum Hall Systems

Jordan Kyriakidis¹, Daniel Loss¹, and A. H. MacDonald²

¹*Department of Physics and Astronomy, University of Basel, Klingelbergstrasse 82, CH-4056 Basel, Switzerland*

²*Department of Physics, Indiana University, Bloomington, IN 47405, U. S. A.*

(April 18, 2018)

Pseudospin solitons in double-layer quantum Hall systems can be introduced by a magnetic field component coplanar with the electrons and can be pinned by applying voltages to external gates. We estimate the temperature below which depinning occurs predominantly via tunneling and calculate low-temperature depinning rates for realistic geometries. We discuss the local changes in charge and current densities and in spectral functions that can be used to detect solitons and observe their temporal evolution.

73.40.Hm, 71.45.-d, 71.10.Pm, 73.40.Gk, 73.40.-c

The study of multicomponent Quantum Hall systems [1] has been enriched by the discovery of a variety of new phases. In double layers, the relevant discrete degrees of freedom are labelled by the electron's layer and spin indices. At Landau level filling factor $\nu = 2$, recent theoretical work predicted several interesting phases [2] in which both layer and spin play a role; the existence of these phases has been confirmed by experiment [3]. The present study is on double-layer systems at filling-factor $\nu = 1$ [4,5]. At this filling factor, the low-energy electron states are spin-polarized and the system has a broken symmetry ground state with spontaneous inter-layer phase coherence [6]. The rich phase diagram for these systems, including the effects of in-plane fields, has been discussed at length in Ref. [5].

It is useful to describe this system using a pseudospin language [4,5] in which pseudospin-up (-down) refers to an electron in the top (bottom) layer. The action is that of a two-dimensional ferromagnet with a hard-axis anisotropy and a Zeeman field perpendicular to the hard-axis [5]. The pseudospin configuration is specified by the spherical-coordinate fields $\theta(x, y)$, which describes the difference in charge density between the layers, and $\phi(x, y)$, which describes the relative phase of electrons in top and bottom layers. Phase solitons $\phi_0(x)$ exist as solutions to the classical equations of motion [5]. In this Letter we address the quantum dynamics of such solitons, predicting that, when pinned by applying gate voltages, depinning occurs at accessible temperatures predominantly via quantum tunneling. This system offers a number of advantages for macroscopic quantum tunneling studies, especially the possibility of using gate voltages and in-plane fields in combination to control metastable-state placement. We also discuss several local properties which can be used to detect solitons and observe their temporal evolution.

Neglecting for the moment the effect of in-plane fields, the leading contributions to the imaginary-time effective action for the pseudospin field $\mathbf{m}(\mathbf{r}, \tau) = (\sin \theta \cos \phi, \sin \theta \sin \phi, \cos \theta)$, in the presence of both tunneling and gates, is given by [5]

$$S^E[\mathbf{m}] = \int d\tau d^2r \left\{ \frac{-i\dot{\mathbf{m}} \cdot \mathbf{A}}{4\pi\ell^2} + \frac{\rho}{2} [(\nabla m_x)^2 + (\nabla m_y)^2] + \beta_0 m_z^2 - \frac{1}{2\pi\ell^2} [tm_x - V(x)m_z] \right\}. \quad (1)$$

The first term is the Berry phase, conveniently expressed as $\dot{\mathbf{m}} \cdot \mathbf{A} = \dot{\phi}(1 - \cos \theta)$. The gradients are the exchange terms, with ρ the pseudospin stiffness. The term involving β_0 is a hard-axis anisotropy, and in the following term, t is the tunneling amplitude which acts as an in-plane pseudofield. Finally, $V(x)$ is the gate potential which can be adjusted *in situ* for appropriately fabricated double-layer samples. The local filling factor for each layer is $\nu_1 = (1 + \cos \theta)/2$, $\nu_2 = (1 - \cos \theta)/2$, with the total filling factor $\nu = \nu_1 + \nu_2 = 1$. The parameters ρ and t in Eq. (1) depend on m_z . We require their expansion to quadratic order in $\vartheta = \theta - \pi/2$, $\rho(m_z) = \rho_0 + \rho_1 \vartheta^2$ and $t(m_z) = t_0 + t_1 \vartheta^2$, and shall use the Hartree-Fock results [7] $\rho_1 = -\rho_0$ and $t_1 = -t_0/2$.

We limit our attention to finite-width (w) systems for which the soliton physics is particularly simple. The flexural bending mode [8,9] of a soliton in the x direction of a two-dimensional system has a spectrum given by $\epsilon(k_y) = 4\pi\ell^2 k_y \sqrt{\rho_0(2\beta_0 + \rho_0 k_y^2)}$, where k_y is the transverse wavevector. The finite-size gap of these modes can be estimated by setting $k_y = \pi/w$. For a given temperature T , the quasi-one-dimensional limit results if flexural modes are frozen out, *i.e.*, if the transverse sample size is smaller than [9] $w(T) = (\pi/\tau)[(\rho_0/\beta_0)(1 + \sqrt{1 + \tau^2})]^{1/2}$, where $\tau = k_B T / (4\pi\ell^2 \beta_0)$. For the sample parameters we give below, $w(1\text{ K}) = 718\text{ nm}$, whereas $w(100\text{ mK}) = 7\text{ }\mu\text{m}$. Assuming the transverse sample size to be less than this value, we can trivially integrate over the y direction.

The estimates for the tunneling rates given below are based on the following [10] parameter values: $2\pi\ell^2\beta_0 \approx 2.3\text{ meV}$, $\rho_0 \approx 0.024\text{ meV}$, $t_0 \approx 0.1\text{ meV}$, and $\ell = 11.8\text{ nm}$. We limit our attention to the regime $V(x) \ll 2\pi\ell^2\beta_0$ and look for solutions to the equations of motion with $\theta = \pi/2$. For $V(x) = 0$, the solution $\phi_0(x - X) = 4 \arctan e^{\pm(x-X)/\delta}$ satisfies the equation of motion, where

$\delta = \sqrt{2\pi\rho_0/t_0}\ell$. The solution ϕ_0 describes a static 2π soliton with width δ centered at position X . The pseudospins rotate in the xy plane by 2π as we move through the soliton, beginning and ending at $\phi_0(\pm\infty) = 0, 2\pi$. Quantum effects are incorporated by expanding about this classical solution, and dynamics is described through a canonical transformation to collective coordinates as we discuss below [9]. We include the effects of the gates self-consistently by substituting the soliton solution $(\theta, \phi) = (\pi/2, \phi_0)$ into the full action. This is valid so long as the soliton energy $E_{\text{soliton}} = 8L_y\rho_0/\delta$ is much larger than the effective potential.

Expanding to quadratic order in $\vartheta(x, \tau) = \theta(x, \tau) - \pi/2$, and performing the functional integral over ϑ (in the partition function), we obtain

$$\frac{S_{\text{eff}}}{L_y} = \int d\tau dx \left[\frac{-i}{4\pi\ell^2} \dot{\phi} + \frac{\rho_0}{2} \left((\partial\phi)^2 + \frac{1}{c^2} \dot{\phi}^2 \right) - \frac{t_0 \cos \phi}{2\pi\ell^2} - \frac{V^2(x)}{a^4\beta_0^2} \left(\rho_0 (\partial\phi)^2 - \frac{t_0 \cos \phi}{2\pi\ell^2} \right) \right], \quad (2)$$

where $c = 2\pi\ell^2\sqrt{8\beta_0\rho_0}$ is the spin-wave velocity. This equation is valid for $t_0/(2\pi\ell^2\beta_0) \ll 1$ and $4\rho_0/(\delta^2\beta_0) \ll 1$. For the parameter values given above, $t_0/(2\pi\ell^2\beta_0) \approx 0.04$ and $4\rho_0/(\delta^2\beta_0) \approx 0.17$.

To describe motion of the soliton, we perform a canonical transformation to collective coordinates. This entails elevating X to a dynamical variable [11,9], $X \rightarrow X(\tau)$, and introducing a constraint to preserve the degrees of freedom. We thus write $\phi(x, \tau) = \phi_0(x - X(\tau)) + \varphi(x - X(\tau), \tau)$ and expand to quadratic order in φ , where ϕ_0 now describes a moving soliton and φ describes a dissipative spin-wave field, which is required to be orthogonal to the zero mode of the soliton field. We incorporate this constraint, explicitly given by $\int dx \phi'_0(x) \varphi(x, \tau) = 0$, via the Fadeev-Popov technique. Briefly, the procedure [9] is to insert into the functional integral the identity $\int \mathcal{D}X \delta(Q) \det(\delta Q/\delta X) \equiv 1$, where $Q[X] = \int dx \phi'_0(x - X) \phi(x, \tau)$. We then expand to second order in both φ and \dot{X}/c . For the bounce solutions considered below, $|\dot{X}/c| \leq 0.26$. This yields a description of the solitons, the spin waves, and the dynamic (non-linear) coupling between them.

Integrating over the spin waves, and including the gate potential, yields an action corresponding to a particle (soliton) at position X , with bare mass M , moving in a potential $\tilde{V}_{\text{eff}}(X)$, with dissipation described by a non-local kernel $K(\tau)$:

$$S_{\text{eff}}[X] = \int_{-\beta/2}^{\beta/2} d\tau \left\{ \frac{1}{2} M \dot{X}^2 + \tilde{V}_{\text{eff}}(X) + \frac{1}{2} \int_0^\tau d\tau' K(\tau - \tau') [X(\tau) - X(\tau')]^2 \right\}. \quad (3)$$

For low temperatures ($k_B T \ll \hbar\omega_0 = 2\hbar c/\delta$), the kernel is given by $K(\tau) = (1/\pi) \int_0^\infty d\omega J(\omega) e^{-\omega|\tau|}$. The spectral

density $J(\omega) = (\omega/\omega_0\delta^2) \sqrt{\omega^2 - \omega_0^2} \Theta(\omega - \omega_0)$ vanishes for $\omega < \omega_0$ (Θ is the step function), and the kernel $K(\tau)$ is exponentially suppressed for $|\tau| > 1/\omega_0$. In the parameter range we are interested in, $k_B T \ll \hbar\omega_b \ll \hbar\omega_0$ (ω_b is the bounce frequency—see below), we can expand $X(\tau) - X(\tau') \approx (\tau - \tau')\dot{X}(\tau')$, and the effect of damping reduces to a renormalization of the soliton mass M . This additive renormalization is intensive with respect to the transverse length L_y of the sample [12], whereas the bare mass is extensive (proportional to L_y), and so we shall not consider this additive piece in what follows. For the estimates we give below, $\omega_b/\omega_0 \leq 0.11$, and $k_B T_C/\hbar\omega_b = 0.47, 0.16, 0.13$, and 0.13 respectively for the entries listed in Table I, where T_C is the crossover temperature (see below).

To leading order, the bare mass is given by $M = \hbar^2 L_y / (4\pi^2 \ell^4 \beta_0 \delta)$, and the effective potential by

$$\tilde{V}_{\text{eff}}(X) = \frac{-3L_y\rho_0}{8(2\pi\ell^2)^2\beta_0^2} \int_{-\infty}^{\infty} dx V^2(x) \left[\partial\phi_0(x - X(\tau)) \right]^2. \quad (4)$$

This effective potential can be understood in terms of the change in the classical soliton energy density when the $m_z = 0$ values for t and ρ in Eq. (1) are replaced by their values at $m_z = -V(x)/4\pi\ell^2\beta_0$, *i.e.*, when the pseudospin polarization produced by the bias potential is accounted for. In Eq. (3), we have neglected phase terms [9]. All such terms vanish for *incoherent* tunneling, as in the case of tunneling out of a metastable state considered below.

To obtain an explicit expression for \tilde{V}_{eff} , we should specify the form of the gate potential $V(x)$. We choose two simple square wells. One applies a gate voltage of $-V_1$ over a width w_1 , $-V_2$ over a width w_2 , and zero voltage elsewhere. The inside edges of the gates are a distance $2x_0$ apart. This yields an effective potential explicitly given by

$$\tilde{V}_{\text{eff}}(X) = v \sum_{i=1}^2 (-1)^i V_i^2 [\tanh \bar{x}_i - \tanh(\bar{x}_i - \bar{w}_i)], \quad (5)$$

where $v = -3L_y\rho_0/[2(2\pi\ell^2)^2\delta\beta_0^2]$, $\bar{x}_i = [X - (-1)^i x_0]/\delta$, and $\bar{w}_i = (-1)^i w_i/\delta$. Self-consistency demands that $E_{\text{soliton}} \gg \tilde{V}_{\text{eff}}$, which places an upper bound on the gate voltage of $V_i^{\text{max}} \approx 2.3 \text{ meV}$.

We will consider tunneling out of metastable states. Once a soliton tunnels out, it does not return. We therefore put $|V_1| < |V_2|$ and $w_1 \ll w_2$. The potential is schematically shown in Fig. 1, with the coordinates shifted as outlined below. The objective is to calculate the tunneling rate out of this metastable state.

It is helpful to shift coordinates so that the metastable minimum is now at the origin and $V_{\text{eff}}(0) = 0$ (See Fig. 1). There is a frequency $\omega_0 = \sqrt{V_{\text{eff}}''(0)/M}$ associated with the curvature of the metastable minimum, and a frequency $\omega_b = \sqrt{V_{\text{eff}}''(X_b)/M}$ associated with the barrier.

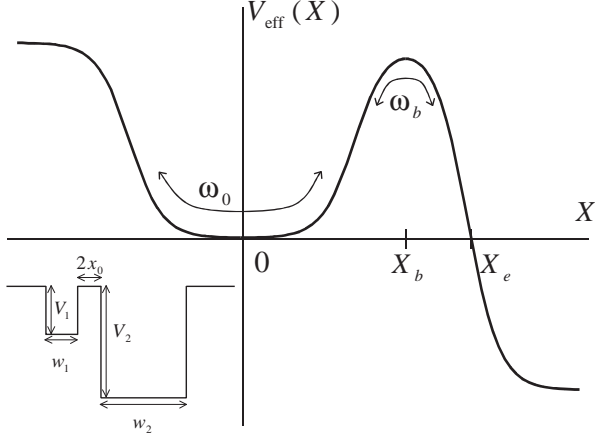


FIG. 1. Effective potential produced by the gate voltages in the “metastable” configuration. The inset shows the “bare” gate potential.

The tunneling rate is given by $\Gamma = K\omega_0 (S_0/2\pi)^{1/2} e^{-S_0}$, where K is a constant whose calculation requires explicit knowledge of the bounce trajectory. The exponent S_0 is the action evaluated along the minimal (bounce) trajectory, which goes from $X = 0$ to $X = X_e$ and back to $X = 0$, while τ goes from $-\beta/2$ to $+\beta/2$, with $\beta \rightarrow \infty$. The crossover temperature T_C defines the boundary between thermally-dominated transitions ($T > T_C$) and tunneling-dominated transitions ($T < T_C$). Both transitions show exponential behavior and one usually assumes that the exponent dominates the prefactor, leading to the expression $k_B T_C = V_{\text{eff}}(X_b)/S_0$.

The tunneling rate, along with the results for the crossover temperature T_C , the classical action S_0 , and the attempt frequency ω_0 are listed in Table I for various gate voltage profiles and transverse sample sizes. These entries were evaluated using the typical model parameters quoted earlier which yield a soliton width of $\delta = 14.5$ nm and a bare soliton mass of $M \approx m^*(0.44L_y/\ell)$, where m^* is the conduction band effective electron mass in GaAs. We conclude from Table I that voltage profiles for which quantum tunneling will dominate at accessible temperatures are achievable with current submicron lithographic technology.

There are at least three properties of pseudospin solitons which should make their existence and their motion experimentally observable: moving solitons disturb the charge balance between the layers; there exists a local electrical current circulating about the axis of the soliton; and the local quasiparticle gap is suppressed in the vicinity of the soliton. These local changes can be detected respectively by electrostatic, magnetic, and tunneling probes of the 2DES. We discuss each briefly.

TABLE I. Tunneling rate Γ , crossover temperature T_C , and attempt frequency ω_0 for several gate widths w_1 , gate separations $2x_0$, and sample sizes L_y . All entries have $w_2 = 400$ nm, $V_1 = -0.75$ meV, and $V_2 = -1.00$ meV, except for the final entry, which also has $V_1 = -1.00$ meV.

L_y [μm]	w_1 [nm]	$2x_0$ [nm]	ω_0 [GHz]	S_0	Γ	T_C [mK]
0.3	100	100	36	12.0	93 kHz	150
0.6	100	50	36	12.5	66 kHz	267
1.0	50	25	187	8.9	63 MHz	367
1.0	20	20	448	5.3	19 GHz	463

That moving solitons transfer charge between layers may be seen by revisiting the classical equations of motion for the action in Eq. (1) and trying to find *moving* soliton solutions. Proceeding in powers of v/c , where v is the soliton velocity and c the spin wave velocity in Eq. (2), we write $\theta_{\text{cl}}(s) = \pi/2 + (v/c)\theta_1(s) + O(v^2/c^2)$ and $\phi_{\text{cl}}(s) = \phi_0(s) + (v/c)\phi_1(s) + O(v^2/c^2)$, where $\phi_0(s)$ is the previous solution for the *static* soliton, and $s = x - v\tau$ is the coordinate of the moving frame. Note that this ansatz satisfies the equations of motion *exactly* for $v = 0$. To linear order in v/c , we find that $\phi_1(s) = 0$, while

$$\theta_1(s) = \frac{\pm(c/2\delta) \text{sech}[(s-s_0)/\delta]}{(a^2\beta_0 + t_0) - 6t_0 \text{sech}^2[(s-s_0)/\delta]}. \quad (6)$$

The local charge transfer produced by the passing soliton is related to the charge transfer produced by the static bias potential which, by virtue of the difference in layer energies it produces, gives the same rate of change of the interlayer phase ϕ . This result shows that whereas a static soliton pseudospin rotates entirely in the xy plane, a *moving soliton pseudospin rises out of the plane* by an amount proportional to the velocity as it undergoes its 2π rotation. This is analogous to closely related models of anisotropic ferromagnets where exact moving soliton solutions are available [13]. In physical terms, a moving soliton transfers charge between the layers, altering the electric potential profile outside of the sample, which can be measured using a scanning single-electron transistor [14]. The total transferred charge for a soliton is given by $Q_e = L_y n e \int dx \cos \theta_{\text{cl}} \approx \mp \pi e n L_y (\dot{X}/c) \sqrt{2\rho_0/\beta}$, with corrections of order $(\dot{X}/c)^2$ and $t_0/(a^2\beta_0)$, and where $n \approx 10^{11} \text{cm}^{-2}$ is the electron density. Using the parameter values given above, a system size of $L_y = 600$ nm, and taking for \dot{X} the maximal velocity along the bounce trajectory, we obtain $|Q_e| \approx 2e$. This value can be increased either by inducing a larger soliton velocity, or by going to a larger sample. These charges should appear, for example, as a soliton tunnels from a metastable state.

Currents, much like those near a vortex in a superconductor, circulate around the axis formed by a soli-

ton line and produce a magnetic field which could in principle be measured. The microscopic operator for the current flowing between layers is the time derivative of the layer-polarization operator in the Heisenberg representation. The only contribution to the commutator comes from the interlayer tunneling term in the microscopic Hamiltonian, and is proportional to the operator for the \hat{y} component of the pseudospin. Taking its expectation value we find for the 3D current between the layers (with the bottom to top layer direction taken as positive) $j_{BT}(x) = -t \sin(\phi_0(x)) / \hbar 2\pi \ell^2$. Currents flow in opposite directions on opposite sides of the soliton. The currents flowing within the bottom (B) and top (T) 2D layers are oppositely directed and given by [5] $j_B(x) = -j_T(x) = \rho \partial \phi_0 / \hbar$. For a stationary soliton these currents satisfy the local charge conservation condition $dj_B(x)/dx = -dj_T(x)/dx = j_{BT}(x)$. The current per unit length flowing around the soliton is $\sim e\rho/\hbar\delta$ and the characteristic loop area of the circulating currents is $\sim d\delta$ where d is the layer separation. For typical parameters, these currents produce a magnetic induction directed along the soliton axis with magnitude $\sim 0.1\mu_B/\ell^2\delta$, which could in principle be detected by a SQUID or with cantilever-based [15] magnetometers.

Microscopic calculations can also be used to evaluate the local gap for charged excitations as a function of position near a stationary soliton. We find [16] that the local gap is always reduced near the soliton center and is given by $E_{\text{gap}}(x) = E_{\text{gap}}(\infty) - 4t(1 - \cos(\phi_0(x)))$. This change in spectral properties might be visible in scanning tunneling probes of 2DES's. This gap suppression is local and will increase the local thermally activated quasiparticle resistivity ρ_{xx} at the soliton center by a factor of $\exp(8t/k_BT) \sim \exp(10/T[\text{Kelvin}])$ which can easily be very large. When a soliton tunnels away from a region defined by a set of voltage probes, we can expect a large signal to be seen in the conductances measured by those probes.

In all of the above, we have assumed the external magnetic field was oriented perpendicular to the layers. But this need not be the case, and it may in fact be preferable to add an in-plane component to the field. In the presence of an in-plane field $\mathbf{B}_{\parallel} = (0, -B_{\parallel}, 0)$, the energy [10] of the soliton is lowered and is given by $E_{\text{sol}} = L_y \rho_0 (8/\delta - 4\pi^2 dB_{\parallel} / \Phi_0)$, where Φ_0 is the flux quantum. The benefit, in the present context, of an in-plane field is that it may be used to thermally create solitons at arbitrarily low-temperatures and thus ensure that solitons exist in the sample.

In summary, we have shown that pseudospin solitons may be pinned and manipulated by applying external gates to the system. One can extend the analysis to the case of a double-well potential, which should exhibit an externally tunable tunnel splitting, and to the case of a periodic potential. The physics in the latter case should be driven by Berry and topological phases, and should be

strongly affected—and possibly controlled—by the gate voltages. This opens the door to a variety of Aharonov-Bohm-type investigations, as well as soliton delocalization and band formation [9]. We have also shown that solitons have an electrical current circulating about their axis, that the local quasiparticle gap is suppressed in the vicinity of the soliton, and also that soliton motion induces a local charge imbalance between the layers. These properties may provide a means through which the soliton dynamics can be experimentally probed.

This work has been supported by the Swiss NSF, and by the US NSF (DMR 97-14055, PHY 94-07194).

-
- [1] B. I. Halperin, *Helv. Phys. Acta* **56**, 75 (1983); A. H. MacDonald, *Surf. Sci.* **229**, 1 (1990); S. M. Girvin and A. H. MacDonald, in *Perspective in Quantum Hall Effects*, edited by S. Das Sarma and A. Pinczuk (Wiley, New York, 1997).
 - [2] L. Zheng, R. J. Radtke, and S. Das Sarma, *Phys. Rev. Lett.* **78**, 2453 (1997); S. Das Sarma, S. Sachdev, and L. Zheng, *Phys. Rev. Lett.* **79**, 917 (1997); S. Das Sarma, S. Sachdev, and L. Zheng, *Phys. Rev. B* **58**, 4672 (1998).
 - [3] V. Pellegrini *et al.*, *Phys. Rev. Lett.* **78**, 310 (1997).
 - [4] A. H. MacDonald, P. M. Platzman, and G. S. Boebinger, *Phys. Rev. Lett.* **65**, 775 (1990).
 - [5] K. Yang *et al.*, *Phys. Rev. Lett.* **72**, 732 (1994); K. Moon *et al.*, *Phys. Rev. B* **51**, 5138 (1995); K. Yang *et al.*, *Phys. Rev. B* **54**, 11644 (1996).
 - [6] S. Q. Murphy *et al.*, *Phys. Rev. Lett.* **72**, 728 (1994); M. B. Santos, L. W. Engel, S. W. Hwang, and M. Shayegan, *Phys. Rev. B* **44**, 5947 (1991); T. S. Lay *et al.*, *Phys. Rev. B* **50**, 17725 (1994).
 - [7] Microscopic evaluation of quantum fluctuation corrections to the Hartree-Fock results for $\rho(m_z)$ and $t(m_z)$ are feasible and would be useful. Once available, these corrections can be used to adjust some of the quantitative estimates made below.
 - [8] J. M. Winter, *Phys. Rev.* **124**, 452 (1962).
 - [9] H.-B. Braun and D. Loss, *Phys. Rev. B* **53**, 3237 (1996).
 - [10] C. B. Hanna, A. H. MacDonald, and S. M. Girvin, *Physica B* **249–251**, 824 (1998), also at cond-mat/9805259.
 - [11] B. Sakita, *Quantum Theory of Many Variable Systems and Fields* (World Scientific, Singapore, 1985).
 - [12] The intensive renormalization arises from the expansion of both \tilde{X} and φ . The first extensive contribution to S_{eff} from the dissipation is at least fourth order in \tilde{X} . For details, see Eqs. (B1) through (B4) of Appendix B in Ref. [9].
 - [13] H.-J. Mikeska, M. Steiner, *Adv. Phys.* **40**, 191 (1991); H.-B. Braun, D. Loss, *Int. J. Mod. Phys. B* **10**, 219 (1996).
 - [14] H. F. Hess, T. A. Fulton, M. J. Yoo, and A. Yacoby, *Solid State Commun.* **107**, 657 (1998); R. C. Ashoori, *Nature* **379**, 413 (1996).
 - [15] J. G. E. Harris *et al.* (to be published).

[16] A. H. MacDonald, J. Kyriakidis, D. Loss, unpublished.

Erratum: Quantum Dynamics of Pseudospin Solitons in Double-Layer Quantum Hall Systems [Phys. Rev. Lett. 83, 1411 (1999)]

Jordan Kyriakidis, Daniel Loss, and A. H. MacDonald
(April 18, 2018)

The expressions, correct to Hartree-Fock order, for the pseudospin stiffness ρ and tunneling amplitude t are given by $\rho = \rho_0$ and $t = t_0$. Consequently, the right-hand side of Eqs. (4) and (5) of our Letter should be multiplied by $1/2$. Some of the entries in Table I are also affected and more representative values are given below. The conclusions and all other results remain unaffected.

TABLE II. Tunneling rate Γ , crossover temperature T_C , and attempt frequency ω_0 for several gate widths w_1 , gate separations $2x_0$, and sample sizes L_y , assuming negligible dissipation (see text). All entries have $w_2 = 400$ nm, $V_1 = -0.75$ meV, and $V_2 = -1.00$ meV, except for the final entry, which also has $V_1 = -1.00$ meV (and the same V_2 and w_2 as the other entries).

L_y	w_1	$2x_0$	ω_0	S_0	Γ	T_C
[μm]	[nm]	[nm]	[GHz]		[KHz]	[mK]
0.6	100	100	26	17.0	0.5	106
1.0	100	50	25	14.7	5	188
2.5	50	25	132	15.8	63	260
2.5	20	20	317	9.4	302	327